NeuroImage 54 (2011) 103–112

Contents lists available at ScienceDirect

NeuroImage

journal homepage: www.elsevier.com/locate/ynimg

Diffusion weighted imaging distinguishes the vegetative state from the minimally conscious state

Davinia Fernández-Espejo [a,*], Tristan Bekinschtein [b], Martin M. Monti [b], John D. Pickard [c], Carme Junque [a], Martin R. Coleman [c], Adrian M. Owen [b]

[a] Department of Psychiatry and Clinical Psychobiology, University of Barcelona, Casanova 143, 08036, Barcelona, Spain
[b] MRC Cognition and Brain Sciences Unit, 15 Chaucer Road, Cambridge, CB2 7EF, UK
[c] Academic Neurosurgery Unit and the Wolfson Brain Imaging Centre, University of Cambridge, Addenbrookes Hospital, Cambridge, CB2 0QQ, UK

ARTICLE INFO

Article history:
Received 2 April 2010
Revised 12 August 2010
Accepted 13 August 2010
Available online 20 August 2010

Keywords:
Vegetative state
Minimally conscious state
Diffusion tensor imaging
Magnetic resonance imaging

ABSTRACT

The vegetative (VS) and minimally conscious (MCS) states are currently distinguished on the basis of exhibited behaviour rather than underlying pathology. Although previous histopathological studies have documented different degrees of diffuse axonal injury as well as damage to the thalami and brainstem regions in VS and MCS, these differences have not been assessed *in vivo,* and therefore, do not provide a measurable pathological marker to aid clinical diagnosis. Currently, the diagnostic decision-making process is highly subjective and prone to error. Indeed, previous work has suggested that up to 43% of patients in this group may be misdiagnosed. We used diffusion tensor imaging (DTI) to study the neuropathology of 25 vegetative and minimally conscious patients *in vivo* and to identify measures that could potentially distinguish the patients in these two groups. Mean diffusivity (MD) maps of the subcortical white matter, brainstem and thalami were generated. The MCS and VS patients differed significantly in subcortical white matter and thalamic regions, but appeared not to differ in the brainstem. Moreover, the DTI results predicted scores on the Coma Recovery Scale ($p<0.001$) and successfully classified the patients in to their appropriate diagnostic categories with an accuracy of 95%. The results suggest that this method may provide an objective and highly accurate method for classifying these challenging patient populations and may therefore complement the behavioural assessment to inform the diagnostic decision making process.

Introduction

The neuropathology of disorders of consciousness (coma, vegetative state, minimally conscious state) has been extensively described at post mortem. Kinney and Samuels (1994) summarised the findings of eleven studies, totalling 178 patients: In patients who had suffered traumatic brain injury leading to impaired consciousness, the most commonly reported damage at post-mortem was diffuse disruption of subcortical white matter, while in patients who had suffered non-traumatic, hypoxic–ischaemic injury, the most commonly reported damage was extensive necrosis in the cerebral cortex. In a later study, Adams et al. (1999) described the post-mortem findings from a series of 35 traumatically brain injured patients considered to fulfil the criteria defining the vegetative state (VS) until the time of their deaths. At post-mortem, diffuse axonal injury and thalamic damage were found to be the most common structural abnormalities, followed by ischaemic brain damage and abnormalities in the brainstem. In a subsequent study, a further 14 patients were included who had suffered hypoxic–ischaemic brain injury (Adams et al., 2000). The most common abnormality in this sub-group was diffuse damage in the neocortex, variable abnormalities in the basal ganglia and cerebellum, severe thalamic damage and minor abnormalities in the brainstem. Jennett et al. (2001) then compared the histopathological findings from the group of VS patients studied by Adams et al. (1999, 2000), with a group of severely disabled patients, including some who were considered to fulfil the criteria defining the minimally conscious state (MCS) before death. The incidence of diffuse axonal injury (grades 2 and 3), and thalamic damage was much less frequent in the MCS group than in the VS group, while brainstem lesions were equally common in the two populations. In a further review, Graham et al. (2005) concluded that, although both VS and MCS arise following diffuse axonal injury with widespread damage to white matter and thalami, the difference between the two populations lies in the severity, rather than the location, of the pathology.

The apparent lack of a pathological distinction between the vegetative and minimally conscious states has created considerable difficulties, clinically and scientifically. Without a clear structural

* Corresponding author. Fax: +34 93 403 52 94.
E-mail addresses: daviniafernandez@ub.edu (D. Fernández-Espejo), tristan.bekinschtein@mrc-cbu.cam.ac.uk (T. Bekinschtein), martin.monti@mrc-cbu.cam.ac.uk (M.M. Monti), jdp1000@wbic.cam.ac.uk (J.D. Pickard), cjunque@ub.edu (C. Junque), mrc30@cam.ac.uk (M.R. Coleman), adrian.owen@mrc-cbu.cam.ac.uk (A.M. Owen).

1053-8119/$ – see front matter © 2010 Elsevier Inc. All rights reserved.
doi:10.1016/j.neuroimage.2010.08.035

marker distinguishing VS from MCS, the differential diagnosis is made on the basis of the patients exhibited behaviour and clinical history. The definition of VS, therefore, describes the behavioural presentation of wakefulness in the absence of any evidence of awareness of self or environment, without any reference to underlying pathology (Jennett and Plum, 1972). A person in VS retains autonomic functions with variable preservation of cranial and spinal reflexes, but exhibits no evidence of sustained, reproducible, purposeful or voluntary behavioural responses to multi-sensory stimulation, nor evidence of language comprehension or response to command (Royal College of Physicians, 2003; Multi Society Task Force, 1994). The definition of MCS is also based on the patient's behaviour, rather than their pathology and requires some reproducible, albeit inconsistent, evidence of awareness of self or environment (Giacino et al., 2002). In practise, MCS describes a spectrum of behaviour which, at its lower boundary requires evidence of visual pursuit and at its upper boundary typically involves intermittent responses to command. Throughout the clinical assessment period, careful and repeated examinations of the patient's spontaneous and elicited behaviour are made, in order to determine whether they have the potential to perceive the external world and to voluntarily interact with it. However, this process is fraught with difficulties and there have been several reports of misdiagnosis, where patients considered to meet the criteria defining VS have been shown to retain some awareness of self or environment when later examined by specialist teams (Andrews et al., 1996; Childs et al., 1993).

Over the past decade, there has been a rapid increase in the number of studies that have used structural and functional brain imaging or electrophysiological investigations in the assessment of patients with disorders of consciousness (Owen et al., 2007). Early metabolic studies using positron emission tomography identified functional disconnections in long-range cortico-cortical and thalamo-cortical pathways (Laureys et al., 1999; Laureys et al., 2000). This work suggested that disorders of consciousness are essentially disconnection syndromes, manifested through a combination of damage to brainstem and thalamo-cortical structures, but did not attempt to distinguish VS from MCS. Morphological studies using magnetic resonance imaging (MRI) have also been conducted, drawing attention to lesions in the thalami and subcortical white matter, as well as evidence of laminar necrosis, brainstem and even dopaminergic nuclear damage (Uzan et al., 2003; Kampfl et al., 1998; Matsuda et al., 2005). The use of different MRI sequences has also been shown to have prognostic utility (Carpentier et al., 2006). For example, by combining morphological information from tradition T2* and FLAIR MRI sequences with spectroscopy, Carpentier et al. (2006) were able to predict which patients were more likely to progress from coma to VS. Functional MRI (fMRI) has also been used to show that the "default" or "resting state" network may predict a patient's subsequent response to stimulation, or indeed, whether they harbour the potential for higher-order cognitive function (Boly et al., 2007). Indeed, activation studies using fMRI have been able to identify residual awareness in a small minority of behaviourally non-responsive patients based solely on their neuronal responses to command (Monti et al., 2010; Owen et al., 2006; for review see Owen and Coleman, 2008). Despite commonalities with post-mortem findings, however, none of this work has been able to identify a pathological measure that will distinguish between VS and MCS, and therefore provide a definitive and objective diagnostic marker that could be combined with behavioural measures in the current clinical protocol.

There is also an extensive EEG literature in patients with disorders of consciousness suggesting that electrocencephalographic early evoked responses to sensory and auditory stimuli can successfully predict a negative outcome from acute comatose or vegetative states (Franck et al., 1985; Fischer et al., 2006), while late event related potentials (mismatch negativity and P300) predict awakening (Daltrozzo et al., 2007; Kotchoubey et al., 2005). Unfortunately, in this patient context, EEG suffers many of the same limitations as fMRI; that is to say, that although there are several good demonstrations that EEG could contribute to the diagnostic process in this patient group, these data are not diagnostically definitive.

Diffusion tensor imaging (DTI) is an emerging technique that complements traditional MRI and may be able to provide erstwhile unavailable information about the pathological substrates of disorders of consciousness. DTI is a modified MRI technique that is sensitive to microscopic, three-dimensional water motion within tissue. In cerebrospinal fluid, water motion is isotropic, i.e., roughly equivalent in all directions. In white matter, however, water diffuses in a highly directional or anisotropic manner. Due to the structure and insulation characteristics of myelinated fibres, water in these white matter bundles is largely restricted to diffusion along the axis of the bundle. DTI can thus be used to calculate two basic properties: the overall amount of diffusion and the anisotropy (Douaud et al., 2007; Benson et al., 2007; Kraus et al., 2007; Ringman et al., 2007; O'Sullivan et al., 2004).

It is only very recently that DTI has been used to evaluate white matter integrity in patients with disorders of consciousness. For example, Voss et al. (2006) described two patients with traumatic brain injury: one who had remained MCS for 6 years and one who had recovered expressive language after 19 years diagnosed as MCS. In both cases, widespread changes in white matter integrity were observed. Interestingly, however, the increased anisotropy and directionality in the bilateral medial parieto-occipital regions that was observed in the second patient reduced to normal values in a follow-up scan performed 18 months later. This coincided with increased metabolic activity, leading the authors to interpret these observations as evidence of axonal regrowth in this region. Although this is certainly a landmark finding in two high spectrum MCS patients, it remains to be seen whether DTI has any diagnostic or prognostic utility in a broader group of patients with disorders of consciousness. To this end, Tollard et al. (2009) and Perlbarg et al. (2009) have recently demonstrated that DTI measures in sub-acute severe traumatic brain injury may be a relevant biomarker for predicting the recovery of consciousness at 1 year. However, VS and MCS patients were classified in the same outcome category and potential differences between these two groups were not investigated. Although, in this context DTI has been generally used to address specific clinical problems, the study of white matter integrity in behaviourally defined states has a more basic relevance to understanding the relationship between brain and behaviour in both health and disease. For example, in healthy volunteers, DTI techniques have been used recently to examine how structural changes underpin the behavioural changes that are related to learning a complex skill (Scholz et al., 2009). In the current study, we focus on a behavioural distinction that is used to infer whether consciousness persists (VS patients are defined by the absence of behavioural evidence of awareness while MCS patients are known to be at least partially aware). Studying the cerebral structural differences between these two groups of patients may therefore lead to a better understanding of the neural architecture that is necessary for conscious awareness in the healthy brain.

Here we describe the diffusion characteristics of two groups of patients meeting the clinical criteria for VS ($n = 10$) and MCS ($n = 15$). We evaluate whether (a) the diffusion characteristics of these patients match those of previous post-mortem work (b) whether DTI measures correlate with the behavioural profile of each patient, and (c) determine whether the diffusion characteristics can distinguish between the VS and MCS patient groups.

Materials and methods

Participants

Twenty-five brain-injured patients (16 male, 9 female; mean 38 years old, range 17–68) of varying aetiology, who met the

Table 1
Clinical and demographic characteristics of the VS and MCS cohort.

Patient	Diagnosis	Age	Sex	Aetiology	Time of scan post ictus (months)
VS1[a]	VS	58	M	Left subdural haemorrhage following assault	6
VS2	VS	50	F	Meningitis followed by cardio-respiratory arrest	8
VS3[a]	VS	39	F	Right subdural haemorrhage following fall	10
VS4	VS	34	M	Anoxic brain injury following cardio-respiratory arrest	10
VS5	VS	68	M	Left fronto-parietal subdural haemorrhage and intracerebral bleeds following road traffic accident.	14
VS6	VS	21	M	Left subdural haemorrhage following assault.	6
VS7	VS	45	M	Left frontal intracerebral haemorrhage following road traffic accident.	3
VS8	VS	41	M	Anoxic brain injury following cardio-respiratory arrest	10
VS9	VS	49	M	Bifrontal subdural haemorrhages following road traffic accident.	4
VS10[b]	VS	48	F	Anoxic brain injury following cardio-respiratory arrest.	18
MCS1[c]	MCS	54	F	Brainstem stroke	5
MCS2	MCS	23	F	Bifrontal contusions and diffuse axonal injury following road traffic accident	14
MCS3	MCS	17	M	Subarachnoid haemorrhage, left frontal lobe contusion and diffuse axonal injury following road traffic accident.	7
MCS4	MCS	65	M	Left temporal lobe contusion and subarachnoid bleed following fall.	6
MCS5	MCS	30	M	Right subdural haematoma and diffuse axonal injury following fall.	11
MCS6	MCS	29	F	Right hemisphere subarachnoid and midbrain intracerebral haemorrhage following road traffic accident.	1
MCS7	MCS	36	F	Left fontal contusion and small bilateral haemorrhagic contusions following road traffic accident.	3
MCS8	MCS	19	M	Depressed skull fracture with underlying contusions and subarachnoid haemorrhage following road traffic accident.	8
MCS9	MCS	57	M	Anoxic brain injury following cardio-respiratory arrest.	6
MCS10	MCS	26	M	Right hemisphere subarachnoid haemorrhage, basal ganglia and diffuse white matter lesions following road traffic accident.	8
MCS11	MCS	19	F	Diffuse axonal injury following road traffic accident.	1
MCS12	MCS	23	M	Diffuse axonal injury, frontal and temporal lobe contusions following road traffic accident.	11
MCS13[b]	MCS	26	M	Right frontal subdural haemorrhage and diffuse axonal injury following road traffic accident.	11
MCS14[b]	MCS	54	F	Anoxic brain injury following cardio-respiratory arrest.	13
MCS15[b]	MCS	21	M	Left extradural haematoma and diffuse axonal injury following road traffic accident.	19

VS = vegetative state; MCS = minimally conscious state; M = male; F = female.
[a] Patients excluded from thalamus analysis.
[b] Patients discarded after pre-processing steps (see Materials and methods).
[c] Patient excluded from brainstem analysis.

criteria (Royal College of Physicians, 2003; Giacino et al., 2002) defining the VS ($n=10$) or the MCS ($n=15$), were recruited from two specialist neurorehabilitation centres in the United Kingdom. Each patient was admitted to a 1-week programme of investigation, which included repeated behavioural assessments employing the Coma Recovery Scale Revised (CRS), (Giacino et al., 2004) a battery of electrophysiology, including multi-lead electroencephalography, visual and auditory evoked potentials, axial T2, proton density, haemosiderin, inversion and diffusion sensitive structural imaging, in addition to functional brain imaging employing visual and auditory cognitive paradigms. The data reported in the current study relate specifically to the behavioural and DTI components of this week-long assessment. However, this cohort of patients have been described previously in several companion behavioural and neuroimaging studies (e.g. Coleman et al., 2007a,b, 2009; Newcombe et al., 2010).

Prior to admission each patient had already been assessed clinically at the referring centre by a specialist team employing the Coma Recovery Scale Revised or the Sensory Modality Assessment and Rehabilitation Technique (SMART, Gill-Thwaites and Munday, 1999). Referrals to the research unit (Addenbrooke's Hospital, Cambridge, UK) were made at varying time intervals following each patient's brain injury (mean 9 months post ictus, range 1–19 months). Table 1 summarises the clinical and demographic characteristics of the two patient groups. The VS cohort included four patients with brain injuries of non-traumatic origin and six patients with brain injuries of traumatic origin. In the MCS cohort, three patients had brain injuries of non-traumatic origin and twelve patients had injuries of traumatic origin.

In order to compare changes in diffusion, a group of twelve neurologically healthy volunteers (5 male, 7 female; mean 35 years old, range 27–40) were assessed with axial T2, proton density, haemosiderin, inversion and diffusion sensitive structural imaging. This study was approved by the Cambridge Research Ethics Committee. Informed written assent was obtained from the appointed "consultee" for each patient, as defined by the Mental Capacity Act (2005); in all cases this was the patient's next of kin. All of the neurologically healthy volunteers gave written informed consent.

Behavioural profile

Patients were repeatedly assessed over five sessions with the CRS (Giacino et al., 2004). Table 2 summarises their highest ranked behaviour in each submodality over the assessment period. These scores were consistent with those acquired at the referring neurorehabilitation centre.

MRI acquisition protocol

Images were acquired using a 3T MRI Magnetom Trio Tim scanner (Siemens Medical Systems, Germany) at the Wolfson Brain Imaging Centre (Addenbrooke's Hospital, Cambridge, UK) using a body coil for RF transmission and a standard 12-channel head coil for signal detection. The imaging protocol included a 3D structural sagittal T1-weighted MP-RAGE (Magnetization Prepared Rapid Gradient Echo) image (TR = 2250 ms; TE = 2.98 ms; matrix size = 256 × 231; flip angle = 9; 160 slices, slice thickness = 1 mm) and an axial diffusion weighted dataset with an echo planar

Table 2
Highest JFK Coma Recovery Scale (CRS) scores for each patient during a 5-day assessment period at the time of MRI investigation.

Patient	Auditory Scale	Visual Scale	Motor Scale	Oromotor/Verbal Scale	Communication Scale	Arousal Scale	Total CRS Score
VS1	2—Localisation to sound	1—Visual startle	2—Flexion withdrawal	1—Oral reflexive movement	0—None	1—Eye opening with stimulation	7
VS2	1—Auditory startle	1—Visual startle	2—Flexion withdrawal	1—Oral reflexive movement	0—None	2—Eye opening without stimulation	7
VS3	1—Auditory startle	0—None	2—Flexion withdrawal	1—Oral reflexive movement	0—None	1—Eye opening with stimulation	5
VS4	1—Auditory startle	1—Visual startle	2—Flexion withdrawal	1—Oral reflexive movement	0—None	1—Eye opening with stimulation	6
VS5	0—None	1—Visual startle	2—Flexion withdrawal	1—Oral reflexive movement	0—None	1—Eye opening with stimulation	5
VS6	1—Auditory startle	1—Visual startle	2—Flexion withdrawal	1—Oral reflexive movement	0—None	1—Eye opening with stimulation	6
VS7	0—None	1—Visual startle	0—None	1—Oral reflexive movement	0—None	1—Eye opening with stimulation	3
VS8	1—Auditory startle	1—Visual startle	2—Flexion withdrawal	2—Vocalisation/oral movement	0—None	2—Eye opening without stimulation	8
VS9	1—Auditory startle	1—Visual startle	2—Flexion withdrawal	1—Oral reflexive movement	0—None	1—Eye opening with stimulation	6
VS10	1—Auditory startle	1—Visual startle	2—Flexion withdrawal	1—Oral reflexive movement	0—None	2—Eye opening without stimulation	7
MCS1	4—Consis movement to command	1—Visual startle	3—Localisation to pain	1—Oral reflexive movement	0—None	2—Eye opening without stimulation	11
MCS2	3—Repro movement to command	5—Object recognition	5—Automatic motor response	1—Oral reflexive movement	0—None	3—Attention	17
MCS3	3—Repro movement to command	3—Pursuit eye movements	2—Flexion withdrawal	2—Vocalisation/oral movement	0—None	2—Eye opening without stimulation	12
MCS4	1—Auditory startle	3—Pursuit eye movements	2—Flexion withdrawal	1—Oral reflexive movement	0—None	2—Eye opening without stimulation	9
MCS5	3—Repro movement to command	3—Pursuit eye movements	2—Flexion withdrawal	1—Oral reflexive movement	0—None	2—Eye opening without stimulation	11
MCS6	1—Auditory startle	3—Pursuit eye movements	2—Flexion withdrawal	0—None	0—None	2—Eye opening without stimulation	8
MCS7	1—Auditory startle	3—Pursuit eye movements	2—Flexion withdrawal	1—Oral reflexive movement	0—None	2—Eye opening without stimulation	9
MCS8	1—Auditory startle	3—Pursuit eye movements	4—Object manipulation	1—Oral reflexive movement	0—None	2—Eye opening without stimulation	11
MCS9	3—Repro movement to command	3—Pursuit eye movements	2—Flexion withdrawal	2—Vocalisation /oral movement	1—Non-functional	2—Eye opening without stimulation	13
MCS10	2—Localisation to sound	3—Pursuit eye movements	2—Flexion withdrawal	1—Oral reflexive movement	0—None	2—Eye opening without stimulation	10
MCS11	2—Localisation to sound	3—Pursuit eye movements	2—Flexion withdrawal	1—Oral reflexive movement	0—None	2—Eye opening without stimulation	10
MCS12	3—Repro movement to command	3—Pursuit eye movements	2—Flexion withdrawal	1—Oral reflexive movement	1—Non-functional	2—Eye opening without stimulation	12
MCS13	2—Localisation to sound	3—Pursuit eye movements	3—Localisation to pain	1—Oral reflexive movement	0—None	2—Eye opening without stimulation	11
MCS14	3—Repro movement to command	2—Fixation	2—Flexion withdrawal	2—Vocalisation /oral movement	0—None	2—Eye opening without stimulation	11
MCS15	1—Auditory startle	3—Pursuit eye movements	2—Flexion withdrawal	1—Oral reflexive movement	0—None	2—Eye opening without stimulation	9

*Auditory scale abbreviation: 4 = Consistent movement to command; 3 = Reproducible movement to command.

imaging sequence (TR = 8300 ms, TE = 98 ms, matrix size = 96 × 96, 63 slices, slice thickness = 2 mm, no gap, flip angle = 90) including diffusion sensitising gradients applied along 12 non-collinear directions using 5 *b* values ranging from 340 to 1590 s/mm^2 and 5 $b = 0$ images. Using multiple *b*-values has been shown to increase the accuracy and repeatability of DTI results (Correia et al., 2009). The medication clinically prescribed for each patient as part of their routine maintenance (which in some cases included muscle relaxants or other mild sedatives) was maintained during the scanning session, but no additional drugs were used.

Data analysis

Diffusion-weighted raw data were visually inspected at the outset to identify any large artefacts, which might subsequently affect the analysis. Four patient datasets (VS10, MCS13, MCS14, MCS15) were discarded due to large motion-related artefacts and three volumes were removed in one patient (MCS3) because they were affected by minor non-motion related artefacts. To ensure that this procedure had no effect on the subsequent analyses, we randomly removed the same number of volumes in four of the healthy participants and compared the results for the complete and shortened datasets. No significant differences were found in the diffusion maps. The images were processed using the FMRIB Software Library [FSL, version 4.1.0; Oxford Centre for Functional MRI of the Brain (FMRIB), UK; http://www.fmrib.ox.ac.uk/fsl/]. The images underwent eddy current distortion correction (Behrens et al., 2003) and skull-stripping, using the Brain Extraction Tool (BET, Smith, 2002). Mean diffusivity (MD) maps for each participant were calculated using the FSL Diffusion Toolbox (FDT, Behrens et al., 2003).

Region of interest masks

T1-weighted data underwent a series of pre-processing steps, which also included skull and non brain tissue removal using BET, global rescaling and linear registration with the T2-weighted (b0)

brain images (Linear Image Registration Tool, FLIRT, Jenkinson et al., 2002). T1-weighted, T2-weighted and MD maps were then reoriented to the AC-PC line by registering them with an orientated b0 image from a healthy volunteer, using 6 degrees of freedom and the mutual information algorithm. The multi-channel automated segmentation algorithm (FMRIB's Automated segmentation tool, FAST, Zhang et al., 2001) was then used to obtain white matter binary masks using T1-weighted and T2-weighted registered images as inputs. White matter masks were visually inspected after segmentation to ensure that grey matter or cerebro-spinal fluid (CSF) voxels were not misclassified as white matter. Where necessary, misclassified voxels were removed using FSLView masking tools. Where poor segmentation of deep grey matter regions was identified, these were manually removed from the white matter (WM) masks. In order to obtain a final subcortical white matter mask, brainstem and cerebellar regions were manually removed. Focal lesions were manually outlined on the T2-weighted images and removed from the WM masks (Fig. 1).

Brainstem masks were manually drawn for each participant using the T2-weighted, MD map and T1-weighted images (all in diffusion space), taking special care to exclude CSF voxels. The same criterion employed by Della Nave et al. (2004) was used to define the upper boundary of the brainstem—a line perpendicular to the cerebral peduncles, traced between the widest portion of the third ventricle, medially, and the lateral surface of the cerebral peduncles, laterally. To ensure that the same area was included in all participants (and because some of the datasets did not include the most basal portion of the brainstem) the lower limit was defined as the second slice after the beginning of the medulla (Fig. 1). One patient with a brainstem stroke (MCS1) was excluded on the basis of this criterion.

Due to poor resolution in infratentorial areas and a desire to avoid partial volume effects, a spherical region of interest (ROI; radius = 8 mm) was used to investigate thalamic diffusion in each participant. This ROI comprised a significant portion of each thalamus in all of the participants (Fig. 1). The centre of the sphere was placed in the rostro-caudal plane at the slice showing the central part of the interthalamic adhesion (massa intermedia). Within this slice, the central voxel was placed at the centre of the approximate ellipsoid defined by the thalamus, ensuring that the limits of the sphere were at least 2 mm (corresponding to at least 1 voxel width) from both the edge of the ventricles and the tissue boundaries demarcating abnormal from normal-appearing white matter. Patients with macrostructural lesions affecting either left or right thalamus (VS1 and VS3) were excluded from this ROI analysis.

Histograms

An in house script running on Matlab 7.5.0 (Natick, MA, USA) was used to generate histograms from the MD maps. White matter and brainstem ROI histograms were generated by allocating the MD values to 250 bins, while thalamic histograms were generated using 100 bins (due to their smaller size). Each bin was normalized to the total number of voxels contributing to the histogram in order to compensate for the variability in brain size. The median, peak height, peak location and peak width were then calculated and used to characterise water motion within the ROIs. The median was used rather than the mean because the distribution of MD was non-Gaussian (Chun et al., 2000).

Statistical analysis

Histogram measures were analyzed using SPSS v14.0. For each measure, differences between groups were investigated using a non-

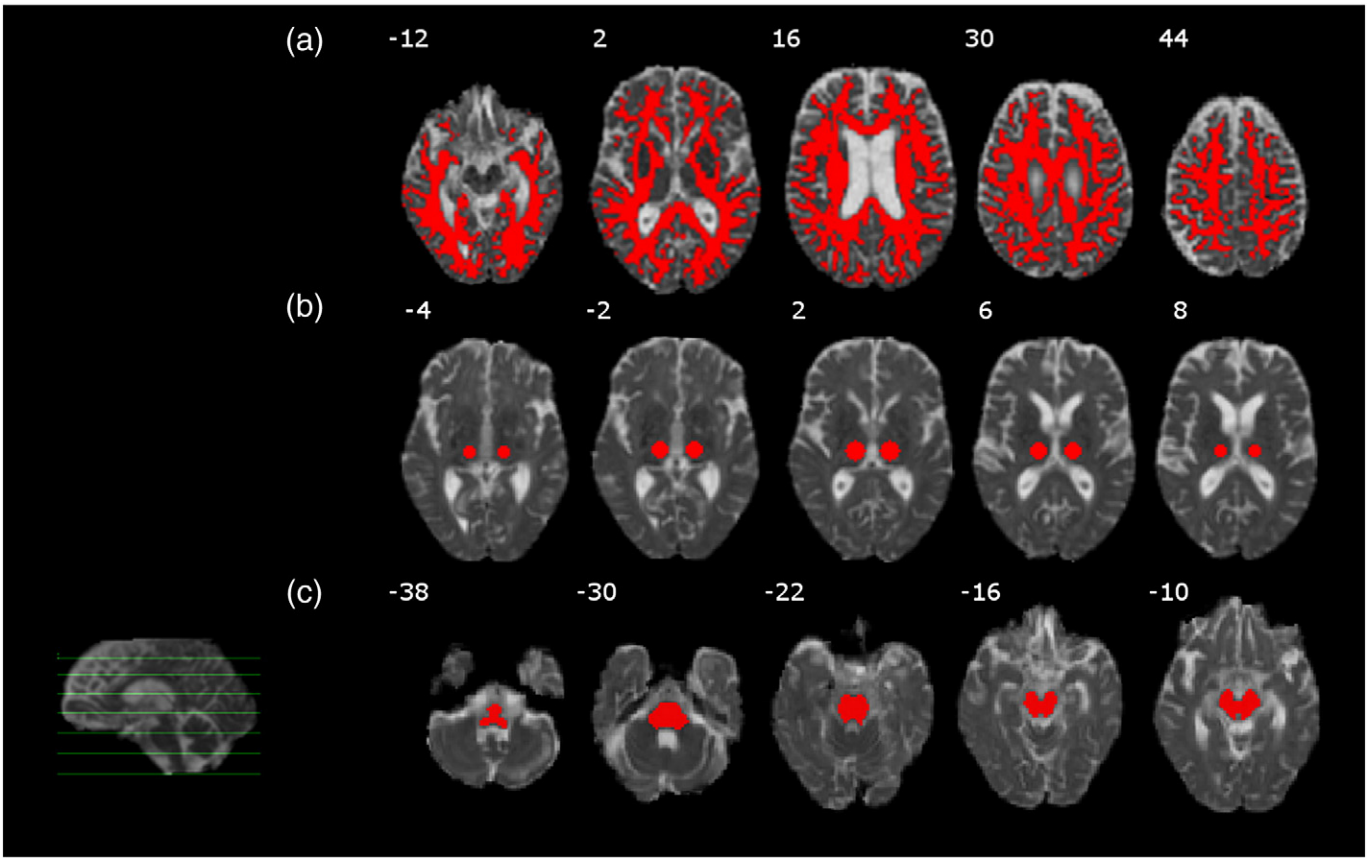

Fig. 1. (a) Subcortical white matter, (b) thalamic, and (c) brainstem ROIs (red shaded areas) superimposed on the mean diffusivity map for patient MCS4. Images displayed in radiological format.

parametric Mann–Whitney *U* Test with an exact (i.e. non-asymptotic) significance assessment method. It has been suggested that this method increases the reliability of results in small sample sets by dispensing with the assumptions required for the asymptotic method (Siegel and Castellan, 1988). For each ROI, two regressions were performed using the measure that produced the greatest effect size when comparing the two patient groups across white matter and thalami. First, a linear regression was used to assess whether thalamic and white matter peak height measures significantly correlated with behavioural measures (i.e. CRS). Second, a binary logistic regression was then employed to test whether neuroanatomical measures could be used to successfully discriminate between the two patient groups. The inclusion of only two factors in the binary logistic regression allowed a ratio of approximately 1 to 10 to be maintained between regressors and observations (Harrell et al., 1984; Peduzzi et al., 1996). The two factors were entered in a single block, using a forward likelihood ratio method. Model significance was assessed with the omnibus χ^2 test. Given the relatively small sample size the Hosmer and Lameshow goodness of fit statistic was also computed, which tests the null hypothesis that the model adequately fits the data. It has been suggested that this latter test is particularly reliable when few observations are available (Hosmer and Lemeshow, 1989). As an additional measure to increase the reliability of the binary logistic regression a repeated 75/25 validation of the results was conducted. Accordingly, across 50 iterations, a subset of 75% of the observations was randomly selected for inclusion in the regression. Then, the significance of the model with this subset of observations was evaluated, as described above. Finally, the model was then applied to the whole sample (i.e. including those observations that were not used to derive the model).

Results

Demographical data

There were no significant differences between patients and healthy participants in terms of age ($U=119.5$, $p=0.808$) or gender ($\chi^2=1.954$, $p=0.162$). There were no significant differences between the MCS and VS groups in terms of age ($U=29$, $p=0.075$), gender ($\chi^2=0.875$, $p=0.350$) time post ictus ($U=46$, $p=0.561$) or distribution of TBI and non-TBI aetiologies ($\chi^2=0.788$, $p=0.375$).

Median MD

An initial analysis of the median MD values for the three ROIs (subcortical white matter, thalami and brainstem) revealed significant differences between the combined patient group and the healthy volunteers in subcortical white matter ($U=0.000$, $p<0.001$, $r=0.82$) and brainstem regions ($U=44$, $p=0.002$, $r=0.52$), but revealed no differences at all between the MCS and VS subgroups (Fig. 2a, b).

Histogram analysis of diffusivity

Patients versus healthy volunteers

A comparison of subcortical white matter histogram indices revealed significant differences in both the VS and the MCS groups in comparison to healthy volunteers. Thus, in both patient groups, peak location and peak width were significantly increased, while the peak height was significantly decreased (Table 3). Similar, but less significant, differences were observed in the brainstem ROI (Table 3). In the thalamic ROI, both MCS and VS patients demonstrated a significant increase in peak width in comparison to healthy volunteers, but only the VS group showed a correspondingly significant decrease in peak height (Table 3).

VS versus MCS patients

When the white matter ROI histogram indices in the VS patients were compared to those of the MCS group, a significant decrease in the peak height was observed ($U=16$, $p=0.006$, $r=0.59$; Fig. 3). A significant decrease in peak height was also found in the thalamic ROI in the VS group ($U=4$, $p<0.001$, $r=0.74$; Fig. 3) accompanied by a significant increase in the peak width ($U=8$, $p=0.003$, $r=0.66$). In contrast, no differences between the VS and MCS groups were found in the brainstem ROI (Table 3).

Because both age and time post ictus are known to be variables that can potentially affect MD values, we further tested the significance of the differences between VS and MCS patients by means of an ANCOVA using age and time post ictus as covariates of no interest. It has been suggested that ANCOVA is robust in the face of deviations from normality or homoscedasticity (Lindman, 1974; Box and Andersen, 1955). No change in the pattern of significant and non-significant differences between groups was observed, i.e., we found significant differences in the white matter peak height ($F_{1,17}=8.707$, $p=0.009$), the thalamic peak height ($F_{1,15}=21.758$ $p<0.001$) and peak width ($F_{1,15}=10.63$, $p=0.005$).

Traumatic versus non-traumatic aetiology

The number of patients included in this study with non-traumatic brain injuries was small ($n=5$), which precluded any meaningful direct comparison between traumatic and non-traumatic cases. Informally, when the histogram measures for the two patient subgroups were compared, they did not appear to differ and, unsurprisingly (given the low power), none reached significance.

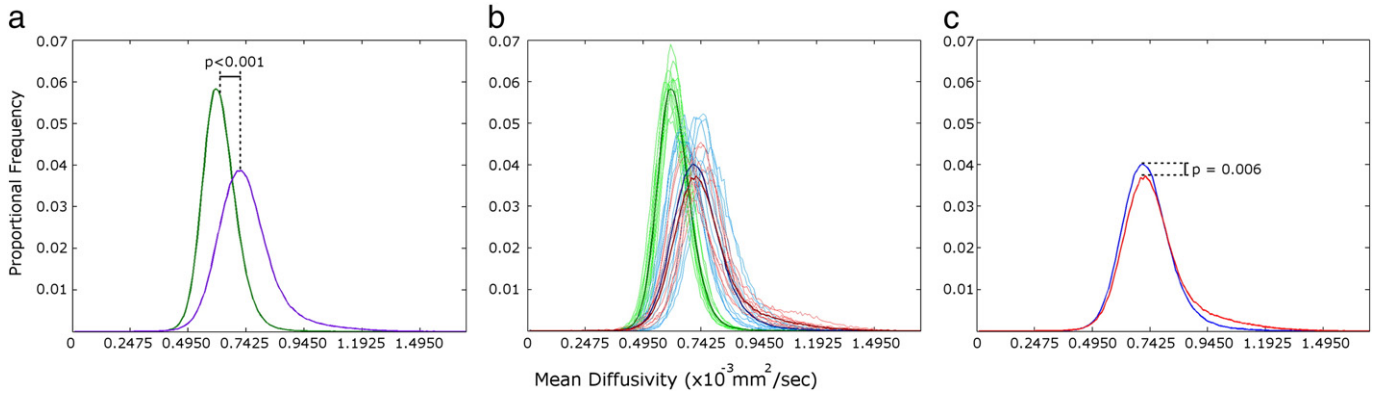

Fig. 2. Subcortical white matter ROI, mean diffusivity histograms: (a) Mean histogram for the control (green) and combined patient (purple) groups. A Mann–Whitney *U* test showed significant differences in the median value between groups; (b) Individual histograms for the control volunteers (green), MCS (blue) and VS (red) patients. The thicker lines represent the mean histogram for each group; (c) Mean histogram for the VS (red) and MCS (blue) groups. A Mann–Whitney *U* test revealed significant differences ($p<0.01$) in the peak height.

Table 3
Histogram summary measures from subcortical white matter, thalami and brainstem regions of interest for healthy control volunteers, VS and MCS patient groups.

ROI	Histogram parameter	Controls	MCS	VS
Subcortical white matter	Median	0.627 ± 0.013	$0.724 \pm 0.049^{a***}$	$0.740 \pm 0.030^{a***}$
	Peak height	0.060 ± 0.005	$0.047 \pm 0.004^{a***}$	$0.041 \pm 0.004^{a***,b**}$
	Peak location	0.616 ± 0.016	$0.712 \pm 0.055^{a***}$	$0.723 \pm 0.036^{a***}$
	Peak width	0.153 ± 0.013	$0.191 \pm 0.018^{a***}$	$0.204 \pm 0.018^{a***}$
Brainstem	Median	0.556 ± 0.034	$0.627 \pm 0.054^{a**}$	$0.604 \pm 0.055^{a*}$
	Peak height	0.066 ± 0.010	$0.052 \pm 0.006^{a**}$	$0.048 \pm 0.007^{a***}$
	Peak location	0.540 ± 0.033	$0.616 \pm 0.049^{a***}$	$0.578 \pm 0.052^{a*}$
	Peak width	0.143 ± 0.022	$0.172 \pm 0.030^{a*}$	$0.174 \pm 0.034^{a*}$
Thalami	Median	0.613 ± 0.028	0.653 ± 0.050	0.623 ± 0.055
	Peak height	0.127 ± 0.015	0.127 ± 0.017	$0.087 \pm 0.019^{a**,b***}$
	Peak location	0.615 ± 0.038	0.657 ± 0.048	0.625 ± 0.075
	Peak width	0.177 ± 0.22	$0.108 \pm 0.027^{a*}$	$0.158 \pm 0.033^{a*,b**}$

All indexes, with the exception of peak height are expressed in $mm^2/s \times 10^{-3}$. Peak height is expressed as a proportion.
Mann–Whitney *U* test:
[a*] $p<0.05$ of the difference between MCS or VS patient group and control group.
[a**] $p<0.01$ of the difference between MCS or VS patient group and control group.
[a***] $p<0.01$ of the difference between MCS or VS patient group and control group.
[b*] $p<0.001$ of the difference between MCS and VS patient groups.
[b**] $p<0.001$ of the difference between MCS and VS patient groups.

Regression analysis

A linear regression analysis revealed that the peak height measure for white matter and thalami significantly predicted the clinical category of patients as defined by their Coma Recovery Scale score ($F_{2,16} = 13.35$, $p<0.001$; $R^2 = 0.63$, Fig. 4). A binary logistic regression in two steps was then undertaken to assess the contribution of each factor. On its own, the thalamic peak height measure performed significantly better than the null model ($\chi^2(1) = 13.82$, $p<0.001$; Nagelkerke-$R^2 = 0.71$; Hosmer and Lameshow $\chi^2(8) = 3.22$, $p = 0.92$) predicting 84.2% of cases correctly. Adding the white matter peak height measure increased the accuracy of the model ($\chi^2(1) = 5.74$, $p = 0.017$; Nagelkerke-$R^2 = 0.88$; Hosmer and Lameshow $\chi^2(8) = 2.79$ $p = 0.95$) such that 94.7% of cases were correctly predicted. Given the relatively small sample size, a 75/25 validation of the binary logistic regression was performed. In every single one of 50 repetitions, a model built from a randomly selected subset of 75% of the observations, generated a result that was significantly better than the null model (with the omnibus χ^2 test ranging from a minimum of 8.14 to a maximum of 16.7), with a prediction accuracy of 90%. When applying the model derived from the subset of 75% of the observations to the full set (i.e. including excluded cases) the prediction accuracy ranged from between 89% and 94%.

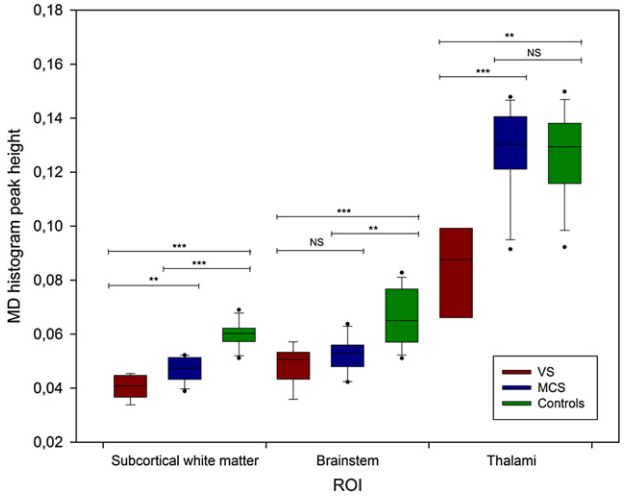

Fig. 3. Boxplot of the peak height values from (a) subcortical white matter, (b) brainstem and (c) thalamic ROIs for the control ($n = 12$), MCS ($n = 12$) and VS ($n = 9$) groups. Mann–Whitney *U* test results are displayed: *** $p<0.001$; ** $p<0.01$; NS: non-significant. Note that one MCS patient was excluded from the brainstem analysis and two VS patients were excluded from the thalamus analysis.

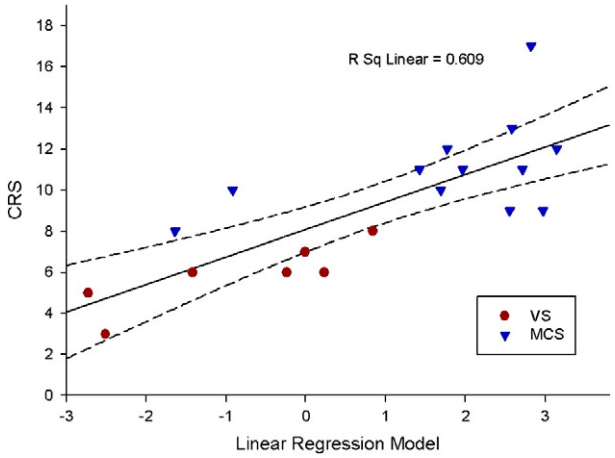

Fig. 4. Linear regression for the combined white matter and thalamic peak heights versus CRS scores. Dashed lines represent 95% confidence intervals.

Discussion

In this study, the integrity of white and grey matter regions was assessed in a group of 25 VS and MCS patients *in vivo*. In accordance with previous post-mortem work (Jennett et al., 2001; Adams et al., 1999) significant changes were observed in the integrity of the tissue in subcortical, thalamic and brainstem regions in the patients when compared to healthy volunteers. The precise location of this damage was not different between the MCS and VS sub-groups, which, again, accords well with previous post-mortem studies. However, an analysis of the MD values within two of these regions of interest (subcortical white matter and thalami), revealed significant differences between the patients meeting the clinical (behavioural) criteria defining VS and those who met the criteria defining MCS. Specifically, the VS patient group exhibited a decrease in the peak height of the histograms derived from the subcortical white matter and the thalami and an increase in the peak width of the thalamic histogram.

Although these *in vivo* differences between the two behaviourally defined patient groups are significant and compelling, the interpretation of DTI data is still very much in its infancy and, as a consequence, the pathological processes that are reflected in these measures can only be speculated upon. In particular, the exact pathological correlate of changes in MD values has not been clearly established. However, it seems likely that histogram peak height provides an index of the remaining healthy tissue (i.e. the proportion of voxels with low MD values). According to this model, a reduced peak MD distribution in the white matter would reflect a greater vulnerability of the fibres with relatively lower MD. In Fig. 2, it is clear that this change (a reduction in peak height) is associated with a larger proportion of voxels with higher MD values. Higher MD values are associated with increases in molecular water displacement, presumably related to the enlargement of extracellular space caused by both axonal injury and demyelination. The thalamic histogram distribution was also less peaked as well as more symmetrical in the VS group (compared to MCS) possibly indicating a greater loss of healthy neurons related to ischaemic necrosis or transneuronal degeneration.

Nevertheless, the central question under investigation here was whether these clinically (i.e. behaviourally) defined sub-groups could

be reliably distinguished purely on the basis of these *in vivo* pathological measures. When the highest effect size measures summarising the change in white matter in subcortical and thalamic regions were taken together, VS and MCS patients could be distinguished reliably and objectively *with 95% accuracy*. To our knowledge, this is the first time that an objective *in vivo* pathological measure has been identified that is able to correctly differentiate between VS and MCS with a high level of accuracy. Such a measure provides valuable additional information which may aid the diagnostic decision-making process, especially when combined with existing behavioural indices. Moreover, it may help to resolve what are often subjective and ambiguous behavioural markers in these patient groups, thereby reducing the high rate misdiagnosis. For example, the linear regression (Fig. 4) shows both a clear relationship between behavioural scores (CRS) and structural markers (from white matter and thalamic histograms) and a clear distinction between those patients who were clinically diagnosed as VS and those who were diagnosed as MCS. The two behaviourally MCS patients (MCS6 and MCS11) who did not clearly fit into this pattern had histogram measures that placed them among the VS group rather than the MCS group. However, it is important to note that unlike all of the other patients, MCS6 and MCS11 were seen within 1 month of ictus, at a less stable, transitory and acute stage and both subsequently progressed to a severely disabled condition. On this basis, it seems likely that their histogram measures reflected a more acute, unstable pathology at the time of scanning, suggesting that this objective method of classification may be most useful in stable patients, at least where differential diagnosis is concerned. Indeed, it has been reported previously that TBI patients can exhibit pathological diffusion values in late subacute states that then recover in the chronic state in those that show neurological improvements (Sidaros et al., 2008). In any case, given the known 40% misdiagnosis rate in this patient group (Andrews et al., 1996; Childs et al., 1993; Schnakers et al., 2009), the fact that only two patients appeared to be "misclassified" by this objective pathological measure is remarkable.

In Jennett and Plum's (1972) seminal paper which first described the VS, the reasons why the condition was defined on the basis of the patient's behaviour, rather than a physio-anatomical abnormality, were discussed in some detail. For the most part, their definition was dictated by a lack of available information. In addition, they sought a definition that could be interpreted easily at the bedside without complex procedures such as EEG or measurements of cerebral blood flow. They acknowledged the work of Strich (1956) and others, who had started to collect post-mortem evidence highlighting lesions in the cerebral cortex and brainstem as possible underlying pathology, but in practical terms they had no means of detecting these lesions *in vivo*. In short, they wanted a diagnostic term that could be agreed at the bedside, but which also invited further clinical and pathological investigation. To this day, the Royal College of Physician guidelines (2003) and those of the American Multi-Society Task Force on PVS (1994) continue to focus on this original bedside (behavioural) definition, despite increasing evidence that techniques such as MRI and EEG could significantly improve the accuracy of the diagnostic process (e.g. Owen et al., 2006; Coleman et al., 2009; Monti et al., 2010). The results of this study add to that evidence by showing that advanced DTI techniques can also categorise patients on an *anatomical* basis with a high degree of accuracy. In line with previous calls for a multimodal approach (e.g. Coleman et al., 2007a, b), therefore, we suggest that this method can be used to complement the existing diagnostic procedure, in combination with a comprehensive behavioural assessment, electrophysiology, structural and functional MRI.

Clinical challenges aside, disorders of consciousness also provide a valuable opportunity for studying the neural mechanisms that underpin normal awareness. For example, studies of resting state brain function in these patients have led to a better understanding of the functional cerebral networks that could form the basis of normal awareness. Such studies have suggested that altered functional connectivity between parietal and frontal areas in the "default-mode network" could be playing an important role in human consciousness (Boly et al., 2009; Vanhaudenhuyse et al., 2010). Functional connectivity can provide partial information about structural connectivity, but precise relationships between regions cannot be determined (Damoiseaux and Greicius, 2009). Our results complement these findings and give further support to those theories that propose that long range cortico-cortical and thalamo-cortical networks support human consciousness. More generally, our results may also guide further studies into the relationship between brain structure and behaviour in healthy populations. For example, the high success of our procedure in identifying differences between two behaviourally defined categories of patients (VS and MCS) suggests that the same approach may be at least equally successful in determining whether structural connectivity underpins the difference between behaviourally-defined categories of healthy individuals. To take one example, IQ is a behaviourally-derived concept, based on the performance of individuals across diverse cognitive tests. While IQ has been studied with functional neuroimaging (e.g. Duncan et al., 2000), it has not, to our knowledge, been studied using structural imaging techniques. If it were to be, one might expect that differences would be small and, if so, sensitive analysis techniques (such as the approach that we describe in this paper) would be required to detect them.

A number of caveats deserve to be mentioned. First, there are different ways to analyse DTI data, including the recently developed tract-based spatial statistics method (TBSS; Smith et al., 2006, 2007) and future work may improve on the current study by adopting some of these techniques. However, the application of voxel-based approaches that require normalization steps may not be possible in patients of the type included in this study because of the high degree of brain atrophy. In contrast, the method described here considers the brain of each patient in native space and, therefore, does not suffer the same constraints. When working in native space on an ROI basis, the standard procedure is usually to average the DTI-derived values for each subject and each ROI and compare them statistically. Such a comparison may not be sensitive enough to detect differences between groups and may also be biased by individual differences in the size of the ROIs between subjects or between groups. The analysis presented here considers the shape of the distribution of the values within the ROI using several descriptors to quantify the diffusion properties. By normalizing the histograms (by dividing their height by the total number of voxels included), our measures are largely independent of the ROIs' size, which rules out possible effects related to different degrees of atrophy in the patients. Analysis of whole brain histograms have been previously performed in other pathologies such as traumatic brain injury (Benson et al., 2007), Parkinson's disease (Tessa et al., 2008) and multiple sclerosis (see Pagani et al., 2007 for a review). Our method benefits from the advantages of histogram analyses while studying target ROIs based on an a priori hypothesis. Accordingly, we were able to successfully discriminate between the two groups of patients and predict their clinical profile with a high level of accuracy.

Second, although the number of patients included in this study was large compared to other neuroimaging reports in this patient group (and larger than any previous DTI-based investigation in disorders of consciousness), the actual number of patients included was relatively small. Decisions in clinical practice must be made with a high confidence level. Our results are promising, but a much larger study will need to be conducted, including a broader range of patients with different aetiologies, in order to evaluate the robustness and generalizability of the method. It may then be possible to use such methods in a clinically routine context on a single subject basis. Thus, by combining DTI biomarkers with other MRI, EEG or behaviourally derived measures, it may be possible to further reduce our misclassification rate, which, although very low, may still be

unacceptable for clinical decision-making purposes. Only then may it be possible to develop an international standard for the assessment of patients with impaired consciousness, with a strong anatomical basis underpinning the classification.

Acknowledgments

The authors are grateful to Dr. Guy Williams, Dr. Virginia Newcombe and Professor David Menon who acquired the healthy volunteer data reported in this study and to the staff of the Wolfson Brain Imaging Centre and Wellcome Trust Clinical Research Facility at Addenbrookes Hospital, Cambridge. We thank Dr. Heidi Johannsen-Berg, Dr. Tim Behrens and Dr. Ian Nimmo-Smith for providing advice about the statistical treatment of DTI data. This work was supported by the National Institute for Health Research Biomedical Research Centre at Cambridge, the UK Department of Health Technology Platform, in addition to grants from the U.K. Medical Research Council (U.1055.01.002.00007.01) and the James S. McDonnell Foundation. DFE was supported by a scholarship from the Spanish Ministry for Education (AP2006-00862). CJ was supported by grant SAF2007-66077 from the Spanish Ministry of Science and Innovation.

References

Adams, J.H., Jennett, B., McLellan, D.R., Murray, L.S., Graham, D.I., 1999. The neuropathology of the vegetative state after head injury. J. Clin. Pathol. 52, 804–806.

Adams, J.H., Graham, D.I., Jennett, B., 2000. The neuropathology of the vegetative state after an acute brain insult. Brain 123, 1327–1338.

Andrews, K., Murphy, L., Munday, R., Littlewood, C., 1996. Misdiagnosis of the vegetative state: retrospective study in a rehabilitation unit. BMJ 313, 13–16.

Behrens, T.E., Woolrich, M.W., Jenkinson, M., Johansen-Berg, H., Nunes, R.G., Clare, S., Matthews, P.M., Brady, J.M., Smith, S.M., 2003. Characterization and propagation of uncertainty in diffusion-weighted MR imaging. Magn. Reson. Med. 50, 1077–1088.

Benson, R., Meda, S., Vasudevan, S., Kou, Z., Govindarajan, K., Hanks, R.A., Millis, S.R., Makki, M., Latif, Z., Coplin, W., Meythaler, J., Haacke, E.M., 2007. Global white matter analysis of diffusion tensor images is predictive of injury severity in traumatic brain injury. J. Neurotrauma 24, 446–459.

Boly, M., Balteau, E., Schnakers, C., Degueldre, C., Moonen, G., Luxen, A., Phillips, C., Peigneux, P., Maquet, P., Laureys, S., 2007. Baseline brain activity fluctuations predict somatosensory perception in humans. Proc. Natl. Acad. Sci. 104, 12187–12192.

Boly, M., Tshibanda, L., Vanhaudenhuyse, A., Noirhomme, Q., Schnakers, C., Ledoux, D., Boveroux, P., Garweg, C., Lambermont, B., Phillips, C., Luxen, A., Moonen, G., Bassetti, C., Maquet, P., Laureys, S., 2009. Functional connectivity in the default network during resting state is preserved in a vegetative but not in a brain dead patient. Hum. Brain Mapp. 30, 2393–2400.

Box, G.E.P., Andersen, S.L., 1955. Permutation theory in the derivation of robust criteria and the study of departures from assumption. J. R. Stat. Soc. B (Stat. Methodol.) 17, 1–34.

Carpentier, A., Galanaud, D., Puybasset, L., Muller, J.C., Lescot, T., Boch, A.L., Riedl, V., Cornu, P., Coriat, P., Dormont, D., van Effenterre, R., 2006. Early morphologic and spectroscopic magnetic resonance in severe traumatic brain injuries can detect "invisible brain stem damage" and predict "vegetative states". J. Neurotrauma 23, 674–685.

Childs, N.L., Mercer, W.N., Childs, H.W., 1993. Accuracy of diagnosis of persistent vegetative state. Neurology 43, 1465–1467.

Chun, T., Filippi, C.G., Zimmerman, R.D., Ulug, A.M., 2000. Diffusion changes in the aging human brain. Am. J. Neuroradiol. 21, 1078–1083.

Coleman, M.R., Owen, A.M., Pickard, J.D., 2007a. Functional imaging and the vegetative state. ACNR 7, 35–36.

Coleman, M.R., Rodd, J.M., Davis, M.H., Johnsrude, I.S., Menon, D.K., Pickard, J.D., Owen, A.M., 2007b. Do vegetative patients retain aspects of language comprehension? Evidence from fMRI. Brain 130, 2494–2507.

Coleman, M.R., Davis, M.H., Rodd, J.M., Robson, T., Ali, A., Owen, A.M., Pickard, J.D., 2009. Towards the routine use of brain imaging to aid the clinical diagnosis of disorders of consciousness. Brain 132, 2541–2552.

Correia, M.M., Carpenter, T.A., Williams, G.B., 2009. Looking for the optimal acquisition scheme given a maximum scan time: are more b-values a waste of time? Magn. Reson. Imaging 27, 163–175.

Daltrozzo, J., Wioland, N., Mutschler, V., Kotchoubey, B., 2007. Predicting coma and other low responsive patients outcome using event-related brain potentials: a meta-analysis. Clin. Neurophysiol. 118, 606–614.

Damoiseaux, J.S., Greicius, M.D., 2009. Greater than the sum of its parts: a review of studies combining structural connectivity and resting-state functional connectivity. Brain Struct. Funct. 213, 525–533.

Della Nave, R., Foresti, S., Tessa, C., Moretti, M., Ginestroni, A., Gavazzi, C., Guerrini, L., Salvi, F., Piacentini, S., Mascalchi, M., 2004. ADC mapping of neurodegeneration in the brainstem and cerebellum of patients with progressive ataxias. Neuroimage 22, 698–705.

Douaud, G., Smith, S., Jenkinson, M., Behrens, T., Johansen-Berg, H., Vickers, J., James, S., Voets, N., Watkins, K., Matthews, P.M., James, A., 2007. Anatomically related grey and white matter abnormalities in adolescent-onset schizophrenia. Brain 130, 2375–2386.

Duncan, J., Seitz, R.J., Kolodny, J., Bor, D., Herzog, H., Ahmed, A., Newell, F.N., Emslie, H., 2000. A neural basis for general intelligence. Science 289, 457–460.

Fischer, C., Luaute, J., Némoz, C., Morlet, D., Kirkorian, G., Mauguière, F., 2006. Improved prediction of awakening or non awakening from severe anoxic coma using tree-based classification analysis. Crit. Care Med. 34, 1520–1524.

Franck, L.M., Furgiuele, T.L., Etheridge Jr., J.E., 1985. Prediction of chronic vegetative state in children using evoked potentials. Neurology 35, 931–934.

Giacino, J.T., Ashwal, S., Childs, N., Cranford, R., Jennett, B., Katz, D.I., Kelly, J.P., Rosenberg, J.H., Whyte, J., Zafonte, R.D., Zasler, N.D., 2002. The minimally conscious state: Definition and diagnostic criteria. Neurology 58, 349–353.

Giacino, J.T., Kalmar, K., Whyte, J., 2004. The JFK coma recovery Scale–Revised: Measurement characteristics and diagnostic utility. Arch. Phys. Med. Rehabil. 85, 2020–2029.

Gill-Thwaites, H., Munday, R., 1999. The Sensory Modality Assessment and Rehabilitation Technique (SMART): A comprehensive and integrated assessment and treatment protocol for the vegetative state and minimally responsive patient. Neuropsychol. Rehabil. 9, 305–320.

Graham, D.I., Adams, J.H., Murray, L.S., Jennett, B., 2005. Neuropathology of the vegetative state after head injury. Neuropsychol. Rehabil. 15, 198–213.

Harrell Jr., F.E., Lee, K.L., Califf, R.M., Pryor, D.B., Rosati, R.A., 1984. Regression modelling strategies for improved prognostic prediction. Stat. Med. 3, 143–152.

Hosmer, D.W., Lemeshow, S., 1989. Applied Logistic Regression. Wiley, New York.

Jenkinson, M., Bannister, P., Brady, M., Smith, S., 2002. Improved optimization for the robust and accurate linear registration and motion correction of brain images. Neuroimage 17, 825–841.

Jennett, B., Plum, F., 1972. Persistent vegetative state after brain damage: A syndrome in search of a name. Lancet 1, 734–737.

Jennett, B., Adams, J.H., Murray, L.S., Graham, D.I., 2001. Neuropathology in vegetative and severely disabled patients after head injury. Neurology 56, 486–490.

Kampfl, A., Franz, G., Aichner, F., Pfausler, B., Haring, H.P., Felber, S., Luz, G., Schocke, M., Schmutzhard, E., 1998. The persistent vegetative state after closed head injury: Clinical and magnetic resonance imaging findings in 42 patients. J. Neurosurg. 88, 809–816.

Kinney, H.C., Samuels, M.A., 1994. Neuropathology of the persistent vegetative state: a review. J. Neuropatholo. Exp. Neurol. 53, 548–558.

Kotchoubey, B., Lang, S., Mezger, G., Schmalohr, D., Schneck, M., Semmler, A., Bostanov, V., Birbaumer, N., 2005. Information processing in severe disorders of consciousness: vegetative state and minimally conscious state. Clin. Neurophysiol. 116, 2441–2453.

Kraus, M.F., Susmaras, T., Caughlin, B.P., Walker, C.J., Sweeney, J.A., Little, D.M., 2007. White matter integrity and cognition in chronic traumatic brain injury: A diffusion tensor imaging study. Brain 130, 2508–2519.

Laureys, S., Lemaire, C., Maquet, P., Phillips, C., Franck, G., 1999. Cerebral metabolism during vegetative state and after recovery to consciousness. J. Neurol. Neurosurg. Psychiatry 67, 121.

Laureys, S., Faymonville, M.E., Luxen, A., Lamy, M., Franck, G., Maquet, P., 2000. Restoration of thalamocortical connectivity after recovery from persistent vegetative state. Lancet 355, 1790–1791.

Lindman, H.R., 1974. Analysis of variance in complex experimental designs. San Francisco: W. H. Freeman & Co. Hillsdale, NJ USA: Erlbaum.

Matsuda, W., Komatsu, Y., Yanaka, K., Matsumura, A., 2005. Levodopa treatment for patients in persistent vegetative or minimally conscious states. Neuropsychol. Rehabil. 15, 414–427.

Mental Capacity Act, 2005. The Stationary Office Limited, United Kingdom.

Monti, M.M., Vanhaudenhuyse, A., Coleman, M.R., Boly, M., Pickard, J.D., Tshibanda, L., Owen, A.M., Laureys, S., 2010. Willful modulation of brain activity in disorders of consciousness. N. Engl. J. Med. 362, 579–589.

Multi-Society Task Force on Persistent Vegetative State, 1994. Medical aspects of the persistent vegetative state. N. Engl. J. Med. 330, 1499–1508 & 1572–1579.

Newcombe, V.F., Williams, G.B., Scoffings, D., Cross, J., Carpenter, T.A., Pickard, J.D., Menon, D.K., 2010. Aetiological differences in neuroanatomy of the vegetative state: insights from diffusion tensor imaging and functional implications. J. Neurol. Neurosurg. Psychiatry 81, 552–561.

O'Sullivan, M., Singhal, S., Charlton, R., Markus, H.S., 2004. Diffusion tensor imaging of thalamus correlates with cognition in CADASIL without dementia. Neurology 62, 702–707.

Owen, A.M., Coleman, M.R., 2008. Functional neuroimaging of the vegetative state. Nat. Rev. Neurosci. 9, 235–243.

Owen, A.M., Coleman, M.R., Boly, M., Davis, M.H., Laureys, S., Pickard, J.D., 2006. Detecting awareness in the vegetative state. Science 303, 1402.

Owen, A.M., Coleman, M.R., Boly, M., Davis, M.H., Laureys, S., Pickard, J.D., 2007. Using functional magnetic resonance imaging to detect covert awareness in the vegetative state. Arch. Neurol. 64, 1098–1102.

Pagani, E., Bammer, R., Horsfield, M.A., Rovaris, M., Gass, A., Ciccarelli, O., Filippi, M., 2007. Diffusion MR imaging in multiple sclerosis: technical aspects and challenges. Am. J. Neuroradiol. 28, 411–420.

Peduzzi, P., Concato, J., Kemper, E., Holford, T.R., Feinsten, A., 1996. A simulation of the number of events per variable in the logistic regression analysis. J. Clin. Epidemiol. 99, 1373–1379.

Perlbarg, V., Puybasset, L., Tollard, E., Lehericy, S., Benali, H., Galanaud, D., 2009. Relation between brain lesion location and clinical outcome in patients with severe traumatic brain injury: A diffusion tensor imaging study using voxel-based approaches. Hum. Brain Mapp. 30, 3924–3933.

Ringman, J.M., O'Neill, J., Geschwind, D., Medina, L., Apostolova, L.G., Rodriguez, Y., Schaffer, B., Varpetian, A., Tseng, B., Ortiz, F., Fitten, J., Cummings, J.L., Bartzokis, G., 2007. Diffusion tensor imaging in preclinical and presymptomatic carriers of familial Alzheimer's disease mutations. Brain 130, 1767–1776.

Royal College of Physicians, 2003. The vegetative state: Guidance on diagnosis and management [Report of a working party]. Clin. Med. 3, 249–254.

Schnakers, C., Vanhaudenhuyse, A., Giacino, J., Ventura, M., Boly, M., Majerus, S., Moonen, G., Laureys, S., 2009. Diagnostic accuracy of the vegetative and minimally conscious state: clinical consensus versus standardized neurobehavioral assessment. BMC Neurol. 21, 9–35.

Scholz, J., Klein, M.C., Behrens, T.E., Johansen-Berg, H., 2009. Training induces changes in white-matter architecture. Nat. Neurosci. 12, 1370–1371.

Sidaros, A., Engberg, A.W., Sidaros, K., Liptrot, M.G., Herning, M., Petersen, P., Paulson, O. B., Jernigan, T.L., Rostrup, E., 2008. Diffusion tensor imaging during recovery from severe traumatic brain injury and relation to clinical outcome: a longitudinal study. Brain 131, 559–572.

Siegel, S., Castellan, N.J., 1988. Non-parametric statistics for the behavioural sciences. McGraw-Hill, New York.

Smith, S.M., 2002. Fast robust automated brain extraction. Hum. Brain Mapp. 17, 143–155.

Smith, S.M., Jenkinson, M., Johansen-Berg, H., Rueckert, D., Nichols, T.E., Mackay, C.E., Watkins, K.E., Ciccarelli, O., Cader, M.Z., Matthews, P.M., Behrens, T.E., 2006. Tract-based spatial statistics: Voxelwise analysis of multi-subject diffusion data. Neuroimage 31, 1487–1505.

Smith, S.M., Johansen-Berg, H., Jenkinson, M., Rueckert, D., Nichols, T.E., Miller, K.L., Robson, M.D., Jones, D.K., Klein, J.C., Bartsch, A.J., Behrens, T.E., 2007. Acquisition and voxelwise analysis of multi-subject diffusion data with tract-based spatial statistics. Nat. Protoc. 2, 499–503.

Strich, S.J., 1956. Diffuse degeneration of cerebral white matter in severe dementia following head injury. J. Neurol. Neurosurg. Psychiatry 19, 163–185.

Tessa, C., Giannelli, M., Della Nave, R., Lucetti, C., Berti, C., Ginestroni, A., Bonuccelli, U., Mascalchi, M., 2008. A whole-brain analysis in de novo Parkinson disease. Am. J. Neuroradiol. 29, 674–680.

Tollard, E., Galanaud, D., Perlbarg, V., Sanchez-Pena, P., Le Fur, Y., Abdennour, L., Cozzone, P., Lehericy, S., Chiras, J., Puybasset, L., 2009. Experience of diffusion tensor imaging and 1H spectroscopy for outcome prediction in severe traumatic brain injury: Preliminary results. Crit. Care Med. 37, 1448–1455.

Uzan, M., Albayram, S., Dashti, S.G., Aydin, S., Hanci, M., Kuday, C., 2003. Thalamic proton magnetic resonance spectroscopy in vegetative state induced by traumatic brain injury. J. Neurol. Neurosurg. Psychiatry 74, 33–38.

Vanhaudenhuyse, A., Noirhomme, Q., Tshibanda, L.J., Bruno, M.A., Boveroux, P., Schnakers, C., Soddu, A., Perlbarg, V., Ledoux, D., Brichant, J.F., Moonen, G., Maquet, P., Greicius, M.D., Laureys, S., Boly, M., 2010. Default network connectivity reflects the level of consciousness in non-communicative brain-damaged patients. Brain 133, 161–171.

Voss, H.U., Uluc, A.M., Dyke, J.P., Watts, R., Kobylarz, E.J., McCandliss, B.D., Heier, L.A., Beattie, B.J., Hamacher, K.A., Vallabhajosula, S., Goldsmith, S.J., Ballon, D., Giacino, J. T., Schiff, N.D., 2006. Possible axonal regrowth in late recovery from the minimally conscious state. J. Clin. Invest. 116, 2005–2011.

Zhang, Y., Brady, M., Smith, S., 2001. Segmentation of brain MR images through a hidden Markov random field model and the expectation-maximization algorithm. IEEE Trans. Med. Imaging 20, 45–57.